RESEARCH ARTICLE

WILEY

# Selective neural coding of object, feature, and geometry spatial cues in humans

Stephen Ramanoël[1,2]  |  Marion Durteste[1]  |  Alice Bizeul[1]  |
Anthony Ozier-Lafontaine[1]  |  Marcia Bécu[1]  |  José-Alain Sahel[1,3,4,5]  |
Christophe Habas[3,6]  |  Angelo Arleo[1]

[1]Sorbonne Université, INSERM, CNRS, Institut de la Vision, Paris, France

[2]Université Côte d'Azur, LAMHESS, Nice, France

[3]CHNO des Quinze-Vingts, INSERM-DGOS CIC 1423, Paris, France

[4]Fondation Ophtalmologique Rothschild, Paris, France

[5]Department of Ophtalmology, The University of Pittsburgh School of Medicine, Pittsburgh, Pennsylvania, USA

[6]Université Versailles St Quentin en Yveline, Paris, France

**Correspondence**
Stephen Ramanoël, Université Côte d'Azur, LAMHESS, Nice, France.
Email: stephen.ramanoel@univ-cotedazur.fr

## Abstract

Orienting in space requires the processing of visual spatial cues. The dominant hypothesis about the brain structures mediating the coding of spatial cues stipulates the existence of a hippocampal-dependent system for the representation of geometry and a striatal-dependent system for the representation of landmarks. However, this dual-system hypothesis is based on paradigms that presented spatial cues conveying either conflicting or ambiguous spatial information and that used the term *landmark* to refer to both discrete three-dimensional objects and wall features. Here, we test the hypothesis of complex activation patterns in the hippocampus and the striatum during visual coding. We also postulate that object-based and feature-based navigation are not equivalent instances of landmark-based navigation. We examined how the neural networks associated with geometry-, object-, and feature-based spatial navigation compared with a control condition in a two-choice behavioral paradigm using fMRI. We showed that the hippocampus was involved in all three types of cue-based navigation, whereas the striatum was more strongly recruited in the presence of geometric cues than object or feature cues. We also found that unique, specific neural signatures were associated with each spatial cue. Object-based navigation elicited a widespread pattern of activity in temporal and occipital regions relative to feature-based navigation. These findings extend the current view of a dual, juxtaposed hippocampal–striatal system for visual spatial coding in humans. They also provide novel insights into the neural networks mediating object versus feature spatial coding, suggesting a need to distinguish these two types of landmarks in the context of human navigation.

**KEYWORDS**
functional MRI, geometry, hippocampus, landmark, navigation, spatial cues, striatum

---

Stephen Ramanoël and Marion Durteste share co-first authorships.

------------------------------------------------------------

# 1 | INTRODUCTION

The ability to navigate in space is fundamental to most daily activities, whether it be choosing the shortest route to work or meeting a friend in a familiar neighborhood. Despite its apparent simplicity, spatial navigation is a highly complex cognitive process that requires the integration of multimodal sensory information, the creation and maintenance of spatial representations in memory, and the manipulation of these representations to guide navigational behavior effectively (Wolbers & Hegarty, 2010). The adequate use of visual spatial cues constitutes an essential aspect of this process in many species, including humans (Ekstrom, 2015; Gouteux et al., 2001; Hermer & Spelke, 1996).

Early studies pointed to landmarks and geometry as distinct types of visual spatial cues used for self-orientation and navigation (Cheng, 1986; Gallistel, 1990). In the literature, the term *landmark* has been used to designate both discrete elements such as objects and buildings and embedded *featural* information such as color and texture (Doeller et al., 2008; Epstein & Vass, 2014; Gouteux & Spelke, 2001; Lowe et al., 2017; Marchette et al., 2015; Sutton et al., 2010; Wolbers & Büchel, 2005). The term *geometry* has been used to refer to the information provided by layouts such as relative lengths, distances, and angles between surfaces. While some argue that such information can only be derived from three-dimensional (3D) extended surfaces, others warrant a more comprehensive definition of geometry that includes the implicit relationships between objects (Cheng, 1986; Gouteux & Spelke, 2001; Learmonth et al., 2008; Lee & Spelke, 2010; Lourenco et al., 2009; Sutton et al., 2012).

The presence of visual spatial cues in an environment enables long-term spatial knowledge by facilitating the formation of cognitive maps (Epstein & Vass, 2014). Landmarks' size, stability and proximity to the goal are among the key factors that determine their validity as anchor points and their use for navigation (Auger et al., 2015; Auger & Maguire, 2018; Stankiewicz & Kalia, 2007). Geometry constitutes a highly stable and indispensable information as it sets the environment boundaries, thus delineating the navigability of a space (Bécu et al., 2020; Keinath et al., 2017; Sheynikhovich et al., 2009). Given the intricacy of spatial navigation abilities in humans, it is perhaps not surprising that an extended neural network encompassing occipital, parietal, temporal and frontal regions is recruited (Epstein et al., 2017; Qiu et al., 2019). Decades of lesion studies and functional magnetic resonance imaging (fMRI) research have established the hippocampus and associated structures of the medial temporal lobe, such as the entorhinal, perirhinal, and parahippocampal cortices, as central nodes of this network (Epstein et al., 2017; Julian et al., 2018; Spiers & Barry, 2015).
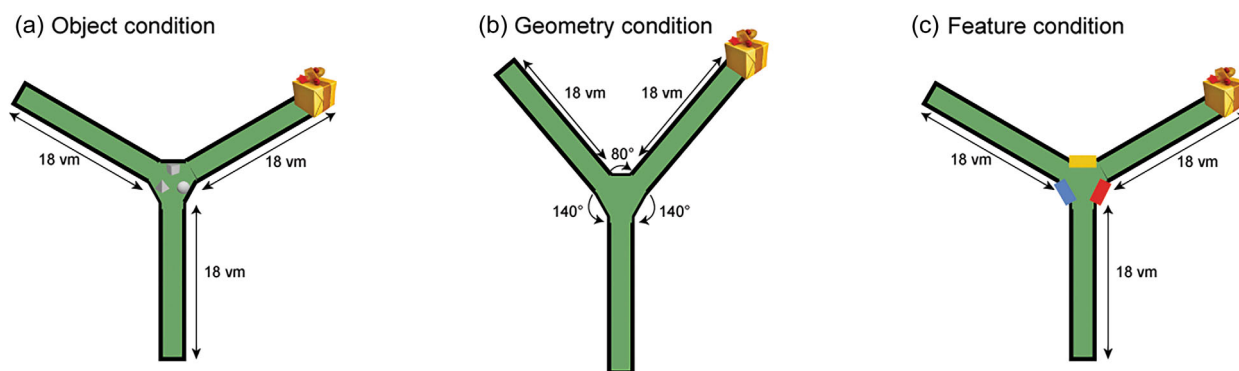
Few experiments exploring the neural underpinnings of human spatial navigation have manipulated the presence of landmark and geometric cues in the environment. In an influential fMRI study by Doeller et al. in which participants had to learn locations relative to a salient object or to a circular enclosure, a striatal-dependent system for the representation of landmarks and a hippocampal-dependent system for the representation of geometry were uncovered (Doeller et al., 2008). This dual-system hypothesis forms the current widespread framework about the neural structures underlying landmark versus geometry spatial coding. However, a limitation of this study lies in the complexity of the paradigm used. In their task both types of visual spatial cues were concomitantly present. Furthermore, reorienting with geometry consisted in integrating positional information between self, the goal, and a distal cue.
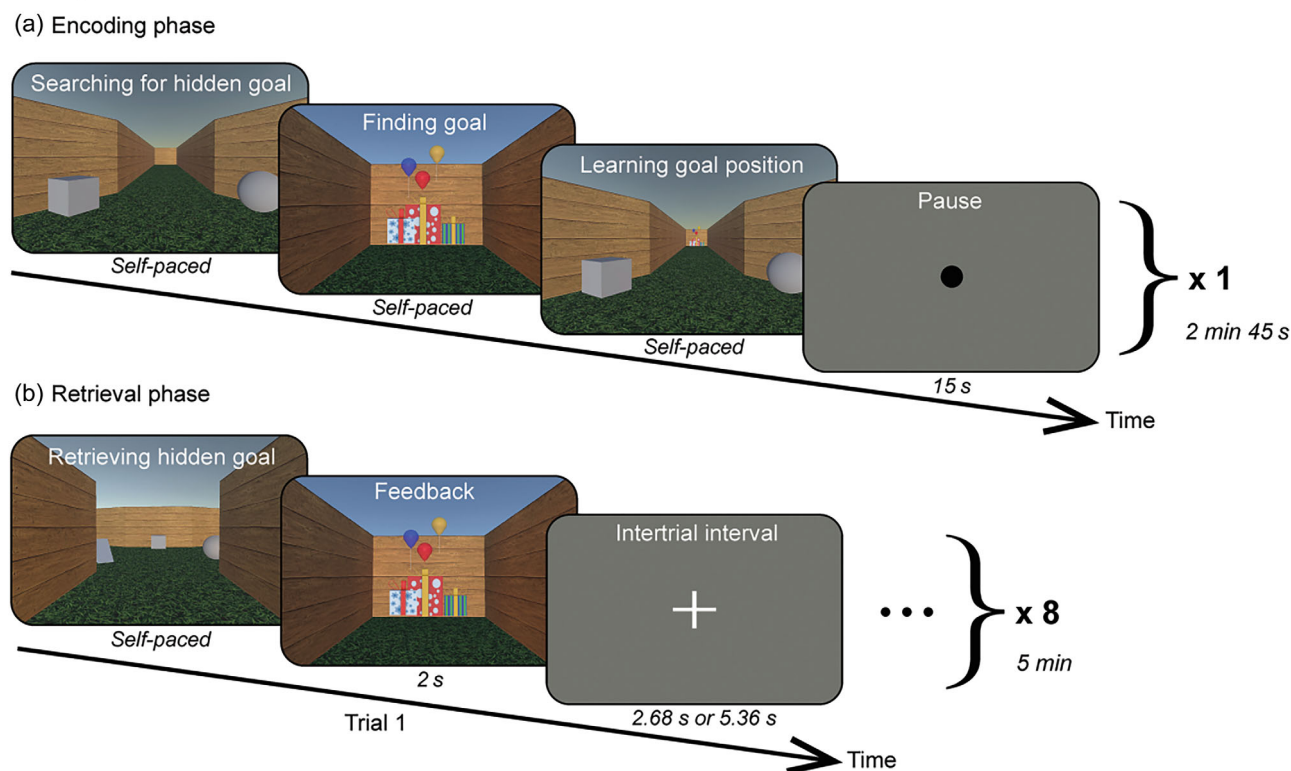
In a subsequent study, Sutton et al. (2010) conducted a fMRI experiment in which participants performed a navigation task within two separate virtual environments that each contained a single orienting cue (Sutton et al., 2010). The authors showed that reorientation based on a featural landmark (colored wall) elicited several activations within the medial temporal lobe whereas reorientation based on geometry (room shape) recruited the prefrontal and inferior temporal cortices. We argue however that the two environments did not allow for a clear dissociation of the neural circuits subtending the use of each cue subtype. Indeed, room size and cue reliance were not made equivalent in the landmark and geometry conditions. While reorienting with the colored wall was unambiguous, reorienting with geometry in the rectangular room was associated with a correct corner and an incorrect rotationally equivalent corner (Forloines et al., 2019; Sutton et al., 2012; Sutton & Newcombe, 2014). Moreover, it is worth noting that while Sutton and colleagues defined landmarks as featural information (colored wall), Doeller et al. defined landmarks as discrete objects independent of the boundaries (vase) (Bullens et al., 2010; Doeller et al., 2008; Doeller & Burgess, 2008). The concept of *landmark* thus seems to vary greatly across studies and deserves clarification.

The inconsistent results mentioned before could originate from the paradigms used (Doeller et al., 2008; Sutton et al., 2010), in which the visual complexity and the ambiguity of the cues (i.e., landmark and geometry provide equivalent spatial information) hindered the possibility to isolate neural circuits for the use of distinct visual spatial cues (Lew, 2011). An alternative nonexclusive explanation lies in the diversity of interpretations regarding the notion of landmark in the literature. The present fMRI study aimed at identifying the specific neural correlates that underlie the processing of objects, features and geometry using an unbiased reorientation navigation task in a virtual maze environment (Figure 1). Specifically, we explored two main questions. First, we tested the validity of the classic framework stating two causally dissociable systems in the hippocampus and striatum. Second, we posited that object-based and feature-based navigation would not be equivalent forms of landmark-based navigation in terms of behavioral and neural markers. We used the term *object* to refer to discrete landmarks that are independent of the environment's boundaries and *feature* to refer to salient information embedded within the boundaries. The virtual environment consisted of a sparse and neutral layout, and the task design allowed for the three different types of visual spatial cues to be clearly separated. We conducted a whole-brain analysis to determine how cerebral regions would be similarly or differentially involved in object, geometry-, and feature-based navigation. Building on the work by Doeller et al. (2008), univariate and multivariate ROI analyses were then performed to elucidate the respective roles of the hippocampus and striatum in cue-based navigation.

## I. Experimental conditions

### (a) Object condition

### (b) Geometry condition

### (c) Feature condition

## II. Task design

### (a) Encoding phase

### (b) Retrieval phase

**FIGURE 1** The virtual navigation paradigm. (I) Schematic overhead perspectives of the virtual environment for the object, geometry, and feature conditions. (a) In the object condition all arms were 18 virtual meters (vm) long and equiangular and three light gray objects were placed in the center of the maze. (b) In the geometry condition the arms were approximately 18 vm long, separated by two 140° angles and one 80° angle and there were no objects in the center of the maze. (c) In the feature condition, the arms were 18 vm long and equiangular, and there were three differently colored walls in the center of the maze. Of note, the overhead perspective was never seen by subjects. (II) The design of one condition. (a) The encoding phase took place only once at the beginning of a condition. Participants were instructed to search for the hidden goal. Once they had found it they needed to learn its position with respect to the available visual spatial cues. A 15-s pause marked the end of the encoding phase. (b) The retrieval phase comprised eight trials. In each trial, participants started from the end of an arm and they needed to retrieve the hidden goal as quickly and as accurately as possible. Each trial was separated by an interval lasting 2.68 or 5.36 s.

## 2 | MATERIALS AND METHODS

### 2.1 | Participants

Twenty-six healthy young adults performed the fMRI experiment, but one participant was excluded due to poor task understanding. The final sample consisted of 25 participants (age 22–32, M = 25.4,

SD = 2.7 years; 7F). Subjects were recruited from the French longitudinal cohort study *SilverSight* established in 2015 at the Vision Institute, Quinze-Vingts National Ophthalmology Hospital, Paris (Lagrené et al., 2019). Participants had no history of neurological or psychiatric disorders, they were right-handed, and they had normal or corrected-to-normal eyesight. Prior to the experimental session, subjects completed a battery of neuropsychological tests including the Mini-Mental

State Examination (MMSE) (Folstein et al., 1975) and computerized versions of the 3D mental rotation test (Vandenberg & Kuse, 1978), the perspective-taking test (Kozhevnikov & Hegarty, 2001) and the Corsi block-tapping task (Corsi, 1973). Notably, the object and control conditions were also analyzed and included as control data in a study on healthy aging (Ramanoël et al., 2020).

All subjects provided written informed consent and the study was approved by the Ethical Committee "CPP Ile de France V" (ID_RCB 2015-A01094-45, CPP No: 16122).

## 2.2 | Experimental design

### 2.2.1 | Object, geometry, and feature definition

We defined objects as salient cues that are independent of the environment's layout, geometry as the elements that are intrinsic to the external limits of a space (i.e., wall lengths and angle sizes) and features as salient information that is embedded within the environment's layout (i.e., color). Worthy of note, the nature of geometric information can be separated into global geometry defined by relative wall lengths, and local geometry defined by angle dimensions (Hupbach & Nadel, 2005; Reichert & Kelly, 2011). As this is a topic of ongoing debate, we chose not to make the distinction.

### 2.2.2 | The virtual navigation task

Participants performed a reorientation task in a virtual environment using an MRI-compatible ergonomic two-grip response device (NordicNeuroLab, Bergen, Norway). They could move forward (thumb press), turn right (right index press), and turn left (left index press). A single finger press was necessary to initiate or stop the movement. The task was projected on a MRI-compatible liquid crystal display monitor (NordicNeuroLab, Bergen, Norway) positioned at the head of the scanner bore. The virtual environment was designed with Unity Engine (Unity Technologies version 2017.4.34f1, https://unity3d.com).

Inside the scanner, participants navigated actively in a Y-maze that consisted of three corridors radiating out from a center and delimited by homogenous wooden-like walls (Figure 1a–c). Forward speed of movement was set at 3 virtual meters (vm)/s and turning speed at 40°/s. Subjects completed three distinct reorientation conditions (object, geometry and feature) and one control condition. In the object condition (OBJ), all arms were 18 vm long and equiangular, and three light gray objects were placed in the center of the maze (Figure 1a). In the geometry condition (GEO), the arms were approximately 18 vm long, separated by two 140° angles and one 80° angle and there were no objects in the center of the maze (Figure 1b). In the feature condition (FEAT), the arms were 18 vm long and equiangular, and there were three differently colored walls in the center of the maze (Figure 1c). In the control condition (CTRL), the arms were 18 vm long and equiangular and the maze did not contain any salient visual spatial cues.

The object, geometry, and feature conditions comprised an encoding phase and a retrieval phase. The encoding phase took place once, at the beginning of a condition, and it lasted 2 min and 45 s. During this phase, participants started from the center of the maze. They had to locate the position of a goal hidden at the end of one of the three arms (gifts and balloons). When they arrived at the correct location, the gifts and balloons appeared and remained visible. Subjects could then use the remaining time to learn and remember the position of the goal with respect to the visual spatial cues available at the intersection. Within a limit of 2 min 45 s, the encoding phase was therefore entirely self-paced.

A 15-s pause separated the encoding phase from the retrieval phase. The retrieval phase of the navigation conditions comprised a total of eight trials. In each trial of the retrieval phase, participants started from the end of an arm that did not contain the goal and they had to retrieve the hidden goal. The starting positions across trials were pseudorandomized between subjects. Once they reached the correct goal location, the gifts and balloons appeared for 2 s. Before the start of the next trial, a fixation screen was presented for 2 or 3 TRs (2.68 or 5.36 s). The timings of the intertrial interval were pseudo-randomly allocated. The maximum allocated time to finish the eight trials of a retrieval phase was 5 min. All participants finished within this time frame, and they were presented with a fixation screen until the remaining time had elapsed. The presentation order of the object, geometry, and feature conditions in each trial was counterbalanced between subjects.

The control condition was always performed after the three cue-based reorientation conditions, and it consisted of a four-trial retrieval phase only. Subjects started from the end of an arm chosen randomly and moved to the center of the environment from where the goal was readily visible. They then navigated toward it. The control condition was designed to account for confounding factors such as motor and simple perceptual aspects of the task. For all conditions, we recorded trial duration and response device use during active navigation. The sole purpose of the response device was to allow participants to freely navigate in space.

## 2.3 | MRI acquisition and data preprocessing

Data were acquired using a 3-Tesla Siemens MAGNETOM Skyra whole-body MRI scanner (Siemens Medical Solutions, Erlangen, Germany) equipped with a 64-channel head coil at the Quinze-Vingts National Ophthalmology Hospital in Paris. T2*-weighted echo-planar imaging (EPI) sequences, optimized to minimize signal dropout in the medial temporal region (Weiskopf et al., 2006) were used for functional image acquisition (voxel size = $3 \times 3 \times 2$ mm, TR/TE/flip angle = 2685 ms/30 ms/90°, interslice gap = 1 mm, slices = 48, matrix size = $74 \times 74$, FOV = $220 \times 220$ mm). Finally, a T1-weighted high-resolution 3D image was obtained using an MPRAGE sequence (voxel size = $1 \times 1 \times 1.2$ mm, TR/TE/IT/flip angle = 2300 ms/2.9 ms/900 ms/9°, matrix size = $256 \times 240 \times 176$).

All subsequent fMRI data analyses were performed using SPM12 release 7487 (Wellcome Department of Imaging Neuroscience, London, UK) and ArtRepair toolbox implemented in MATLAB R2015 (Mathworks Inc., Natick, Massachusetts). To ensure state equilibrium, the first five functional volumes from each run were removed. Slice-timing correction and spatial realignment were applied before correcting for motion-related artifacts with ArtRepair. Volumes displaying elevated global intensity (fluctuation >1.3%) and movement exceeding 0.5 mm/TR were repaired using interpolation from adjacent scans. The next preprocessing steps included co-registration with the T1-weighted anatomical scans, normalization to the Montreal Neurological Institute (MNI) space, and spatial smoothing with an 8 mm full-width half maximum (FWHM) Gaussian kernel.

## 2.4 | Statistical analyses

### 2.4.1 | Behavioral analyses

Repeated-measures ANOVA and $\chi^2$ tests were used to compare navigation performance across conditions, including success rate and navigation time. The potential impact of trial number on navigation performance was explored using a linear mixed model that included trial and cue-based condition and their interaction as fixed factors and subjects as random intercepts. Finally, associations between navigation time and scores on various neuropsychological measures were computed using Spearman rank correlations and a linear mixed model that included the interactions between cue-based condition and 3D rotation score, perspective taking score, Corsi forward score, and Corsi backward score as fixed effects and subjects as random intercepts.

### 2.4.2 | Whole-brain analyses

The general linear model (GLM) was used for block design for statistical analysis of fMRI data (Friston et al., 1995). Eight trials of the retrieval phase in the object condition, eight trials of the retrieval phase in the geometry condition, eight trials of the retrieval phase in the feature condition, four trials of the control condition, and fixation times were modeled as regressors, constructed as box-car functions and convolved with the SPM hemodynamic response function (HRF). The encoding phases were not taken into account as the time required to find the goal for the first time differed greatly between participants (Figure S1). Navigation time, response device use during active navigation as well as six movement parameters derived from the realignment correction (three translations, three rotations) were entered in the design matrix as covariates. Time series for each voxel were high-pass filtered (1/128 Hz cut-off) to remove low-frequency noise and signal drift. FMRI contrasts [OBJ > CTRL], [GEO > CTRL], and [FEAT > CTRL] were fed into a group-level one sample $t$-test to compute average activation maps. In addition, direct comparisons between the cue-based conditions were performed. The statistical threshold was set at $p = .001$ uncorrected with a minimum cluster extent of $k = 10$ voxels.

We also conducted a conjunction analysis to map the brain regions that were similarly activated in all three cue-based conditions. Conjunction was performed using the intersection of supra-threshold voxels for the three separate one-sample $t$-tests using a minimal extended threshold set at 10 voxels. Using a similar approach, we then performed a conjunction analysis for each pair of visual spatial cue type.

### 2.4.3 | Region-of-interest analyses

*Univariate analyses*

The hippocampus and striatum (caudate and putamen nuclei) were defined from the AAL probabilistic brain atlas (Tzourio-Mazoyer et al., 2002). Mean fMRI parameter estimates for the contrasts [OBJ > CTRL], [GEO > CTRL], and [FEAT > CTRL] were extracted from the hippocampus and the striatum using the REX MATLAB-based toolkit. A two-way ANOVA was then performed to study the main effects and interactions of ROI (hippocampus and striatum) and condition (object, geometry, and feature) on fMRI parameter activity. To control for a putative learning effect during the retrieval phase, mean parameter estimates in the hippocampus and striatum were also extracted across trial numbers in the object condition using the following contrasts: [OBJ t1 > CTRL t1], [OBJ t2 > CTRL t2], [OBJ t3 > CTRL t3], [OBJ t4 > CTRL t4], [OBJ t5 > CTRL t4], [OBJ t6 > CTRL t4], [OBJ t7 > CTRL t4], and [OBJ t8 > CTRL t4]. The same analyses were conducted for the geometry and feature conditions. Finally, based on several reports suggesting functional differences along the antero-posterior axis of the hippocampus (Dalton et al., 2019; Zeidman & Maguire, 2016), we conducted complementary analyses on the anterior hippocampus (aHC) and posterior hippocampus (pHC) delineated from the Human Brainnetome Atlas (Fan et al., 2016).

*Multivariate analyses*

We used representational similarity analysis to further characterize the roles of the hippocampus and striatum in discriminating between the three types of spatial cues. We first re-estimated the aforementioned GLM (see Section 2.4.2) on unsmoothed data. The fMR signal was extracted from the two pre-defined ROIs and averaged across trials of each unique condition. For each subject, we then constructed representational similarity matrices (RSMs) by calculating pairwise Pearson correlations between each multivoxel pattern of activity from the object, geometry, and feature conditions. We thus obtained symmetric $3 \times 3$ matrices for the hippocampus and striatum with off-diagonal values specifying the neural similarity between each pair of conditions. One-sample permutation tests were performed on the average RSMs to test whether the pairwise correlation coefficients were significantly different from zero. To explore the differences in pattern similarity between the hippocampus and the striatum we conducted a linear mixed-effects model. The lower triangular correlation

coefficients of each RSM were Fisher-$z$ transformed and included as the dependent variable in the model with ROI, condition pair and their interaction as fixed effects and a random intercept for participants. In order to further test the existence of two dissociable systems in the HC and striatum for the processing of geometry and objects, respectively, two theoretical RSMs were constructed. The object and geometry RSMs were created as binary RSMs based on whether one type of spatial cue would be preferentially processed in a ROI (1 was assigned to highly similar pairs of conditions and 0 to highly dissimilar pairs of conditions). Separate linear mixed-effects models were performed to compare the lower triangular correlation coefficients of the theoretical and neural RSMs. For each theoretical RSM, the neural similarity values were included as the dependent variable with the spatial cue similarities included as fixed effects and participants as random intercepts. All the above-mentioned analyses were conducted using the nltools and netneurotools packages and custom code in Python except for the linear mixed-effects models which were performed using the lme4 package in R.
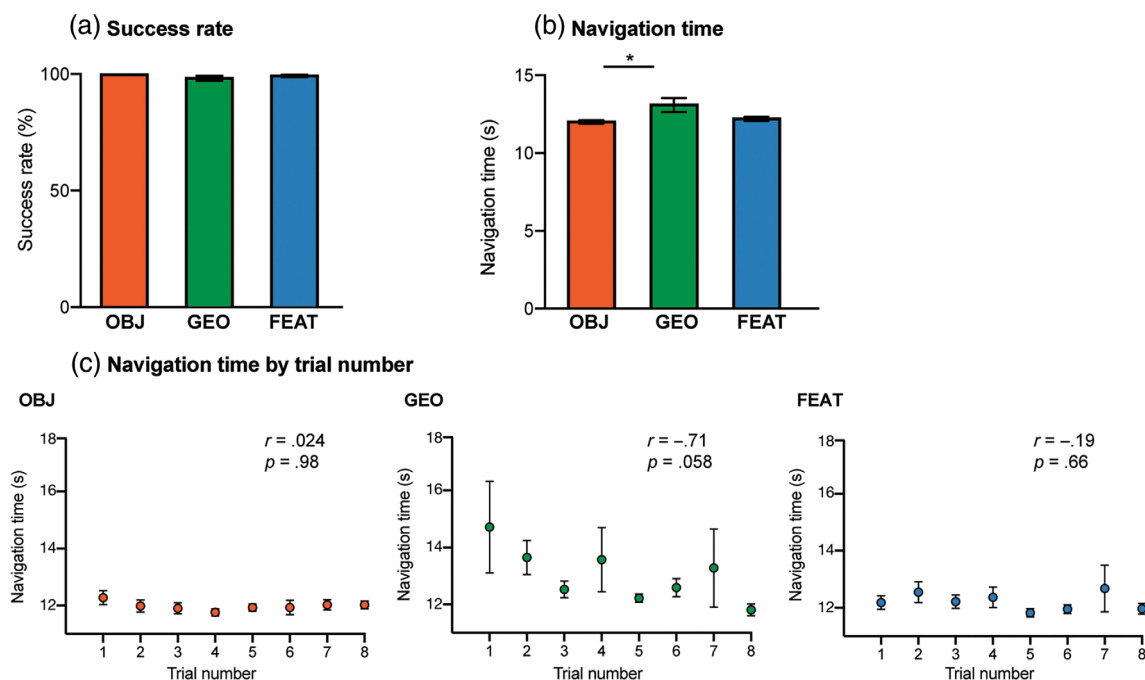
## 3 | RESULTS

### 3.1 | Behavioral results

Success rate (i.e., the number of times a participant chose the correct corridor across trials) was equivalent in the three cue-based conditions (Figure 2a,b). We reported significant differences in navigation time (i.e., time to reach the goal averaged across trials) between conditions ($F(2, 24) = 5.55$, $p = .023$, partial $\eta^2 = 0.32$, 95% CI [0.02, 0.52]). Tukey post hoc tests revealed that young adults took significantly longer to find the goal in the geometry condition than in the object condition ($p = .031$). There were no significant differences in navigation time by trial number across conditions ($F = 1.87$, $p = .073$) lending support to the idea that participants displayed optimal performance from the first trial (Figure 2c). Moreover, trial number was not correlated with navigation time in any of the object ($r = .024$ [$-0.80$, $0.85$], $p = .98$), geometry ($r = -.71$ [$-1.00$, $0.14$], $p = .058$), and feature ($r = -.19$ [$-0.82$, $0.74$], $p = .66$) conditions. We can nonetheless note that navigation time seemed to decrease across trials of the geometry condition. Finally, we found that performance on the perspective-taking task had a significant effect on navigation time independent of the cue-based condition ($0.07 \pm 0.02$, $t = 3.17$, $p = .002$).

### 3.2 | Whole-brain results

For all analyses, the navigation conditions were contrasted to the control condition using the fMRI contrasts [OBJ > CTRL], [GEO > CTRL] and [FEAT > CTRL]. We first conducted a conjunction analysis to explore the cerebral regions commonly activated by the three aforementioned contrasts (Table 1 and Figure S2). We reported significant activations in right anterior cingulate and right inferior temporal gyri. We then investigated the shared clusters of activation for each pair of visual spatial cues (Table 1). The object and geometry conditions both



**FIGURE 2** Behavioral results for the virtual navigation task across cue-based conditions. (a) Proportion of trials in which the correct corridor was chosen (success rate). (b) Time taken to reach the goal averaged across eight trials (navigation time). (c) Navigation time across trial number for the object condition (OBJ), geometry condition (GEO) and feature condition (FEAT). The $r$ and $p$-values correspond to Spearman rank correlations (top right). All error bars represent standard errors of the mean.

**TABLE 1** Cerebral regions whose activity was elicited by the conjunction analyses between the three cue-based conditions contrasted to the control condition and between each pair of conditions contrasted to the control condition.

| Conjunction analysis | H | BA | k | x | y | z |
|---|---|---|---|---|---|---|
| [OBJ ∩ GEO ∩ FEAT] | | | | | | |
| Inferior temporal gyrus | R | 37 | 13 | 42 | −55 | −10 |
| Anterior cingulate gyrus | R | 24 | 11 | 6 | 34 | 4 |
| [OBJ ∩ GEO] | | | | | | |
| Fusiform gyrus | L | 18 | 41 | −26 | −92 | −10 |
| Fusiform gyrus | R | 18 | 39 | 33 | −87 | −8 |
| Anterior cingulate gyrus | R | 24 | 19 | 4 | 32 | 2 |
| Inferior temporal gyrus | R | 37 | 17 | 42 | −61 | −10 |
| Middle temporal gyrus | R | 37 | 11 | 43 | −55 | 10 |
| [OBJ ∩ FEAT] | | | | | | |
| Inferior temporal gyrus | R | 37 | 27 | 41 | −60 | −11 |
| Fusiform gyrus | R | 19 | 13 | 33 | −84 | −13 |
| Cerebellum | R | | 11 | 30 | −55 | −43 |
| Anterior cingulate gyrus | R | 24 | 11 | 9 | 32 | 2 |
| [GEO ∩ FEAT] | | | | | | |
| Anterior cingulate gyrus | R | 24 | 35 | 9 | 32 | 4 |
| Inferior temporal gyrus | R | 37 | 16 | 42 | −64 | −10 |

*Note*: The statistical threshold was defined as *p* < .001 uncorrected for multiple comparisons with an extent voxel threshold defined as 10 voxels. Montreal neurological institute (MNI) coordinates (*x, y, z*) of the peak and number of voxels (*k*) of clusters are also shown.

Abbreviations: BA, Brodmann area; CTRL, control condition; FEAT, feature condition; GEO, geometry condition; H, hemisphere; L, left; OBJ, object condition; R, right.

elicited activity in the fusiform gyrus bilaterally and in the right middle temporal gyrus while the object and feature conditions yielded activity in the right fusiform gyrus and in the right cerebellum. Of note, the conjunction analysis for the geometry and feature conditions showed no additional activation when compared with the main conjunction analysis that included the three conditions.

Next, we were interested in differentiating the neural correlates associated with the use of objects, geometry, and features for spatial navigation. To this end, we looked at the fMRI contrasts [OBJ > CTRL], [GEO > CTRL] and [FEAT > CTRL] separately (Figure 3a–c and Tables S2–S4). The object and geometry conditions ([OBJ > CTRL] and [GEO > CTRL]) elicited activity in bilateral superior temporal and right angular gyri. While the latter two conditions also elicited activation of the bilateral inferior occipital gyrus, the feature condition ([FEAT > CTRL]) yielded a significant cluster in the right inferior occipital gyrus. The geometry and feature conditions both elicited activity in the right superior frontal gyrus. Furthermore, we observed that left hippocampal and left inferior frontal activity were shared by both the object and feature conditions. Finally, multiple areas of the right cerebellum were found to be active in all three conditions.

Examining the individual fMRI contrasts further revealed that each condition had specificities in its pattern of brain activity.

The object condition elicited specific activations of bilateral middle occipital gyri and of the left lateral orbitofrontal gyrus. Moreover, the inferior temporal activity observed throughout the conditions comprised the anterior temporal pole only during object-based navigation. For the geometry condition, we noted extended activations in the frontal cortex encompassing clusters in the left superior frontal gyrus and left precentral gyrus. Geometry-dependent activations were also uncovered in the temporal lobes including the left parahippocampal gyrus and the left middle temporal gyrus, and in the right thalamus. The feature condition yielded activity in the left postcentral gyrus. Notably, the reverse fMRI contrasts, comparing the control condition with each navigation condition, did not reveal any significant activation (Tables S2–S4).

Finally, we conducted direct comparisons between the cue-based conditions themselves. Contrasting the geometry condition with the object condition ([GEO > OBJ]) elicited activity around the left superior frontal gyrus, extending to the left precentral gyrus (main cluster: −30, −10, 62), left caudate nucleus, left cerebellum and brainstem (Figure 4a and Table S5). In addition, when contrasting the geometry condition with the feature condition ([GEO > FEAT]), we found significant activations in the bilateral middle temporal gyrus, middle frontal gyrus and putamen. We also reported activity in the left inferior occipital gyrus and left superior parietal gyrus as well as in the right supramarginal gyrus (Figure 4b and Table S5). The fMRI contrasts comparing the object condition and feature condition with the other conditions ([OBJ > GEO], [OBJ > FEAT], [FEAT > OBJ], [FEAT > GEO]) did not elicit any significant activation (Table S5).

## 3.3 | Regions-of-interest results

A repeated-measures two-way ANOVA was performed with ROI and condition as factors using the fMRI contrasts [OBJ > CTRL], [GEO > CTRL] and [FEAT > CTRL]. There were no main effects of ROI ($F(1, 24) = 1.84$, $p = .19$, partial $\eta^2 = 0.071$, 95% CI [0.00, 0.30]) or condition ($F(2, 48) = 1.56$, $p = .22$, partial $\eta^2 = 0.061$, 95% CI [0.00, 0.20]) on parameter estimates (Figure 5a). A significant interaction between ROI and condition was unveiled ($F(2, 48) = 5.45$, $p = .007$, partial $\eta^2 = 0.19$, 95% CI [0.02, 0.35]). Post hoc tests revealed that the hippocampus was more activated than the striatum in the object condition ($0.40 \pm 0.13$ vs. $-0.09 \pm 0.11$, $p = .016$, Hedge's $g = 0.48$, 95% CI [0.06, 0.91]) and that there was decreased striatal activity in the object condition compared with the geometry condition ($-0.09 \pm 0.11$ vs. $0.46 \pm 0.22$, $p = .005$, Hedge's $g = -0.54$, 95% CI [−0.97, −0.12]).

We observed the hippocampus to be implicated in all cue conditions when compared with the control condition, in varying degrees, and the striatum to be engaged solely during the geometry condition. In order to identify putative learning effects, we examined fMRI parameter activity in individual trials for the contrasts [OBJ > CTRL], [GEO > CTRL], and [FEAT > CTRL]. There were no significant differences in hippocampal and striatal activity between trials for object, feature, or geometry conditions (Figure 5c). We also conducted Spearman
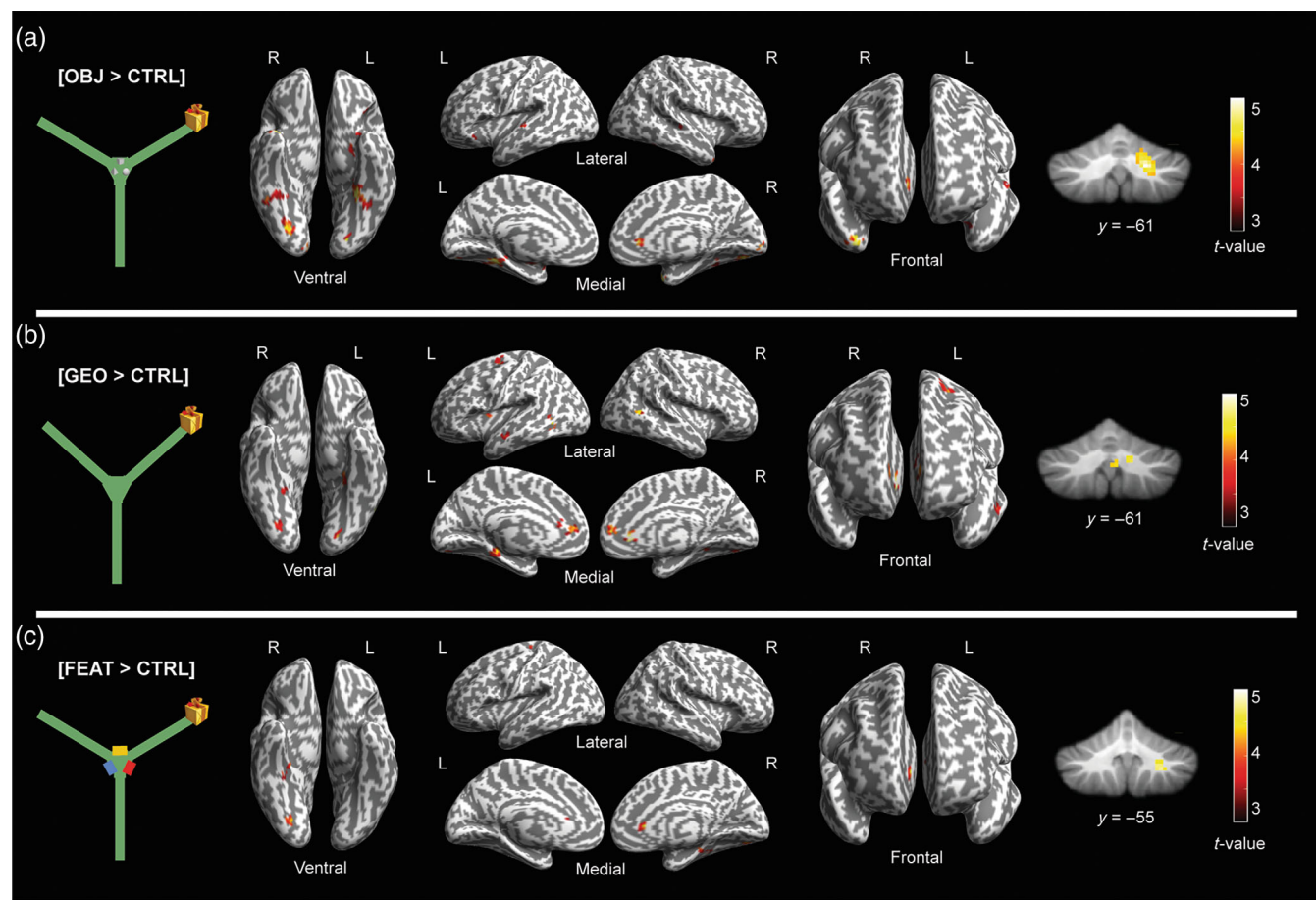
**FIGURE 3** Cerebral regions whose activity was elicited by contrasting (a) the object condition with the control condition [OBJ > CTRL], (b) the geometry condition with the control condition [GEO > CTRL], and (c) the feature condition with the control condition [FEAT > CTRL]. The neural activity is projected onto 3D inflated anatomical templates and 2D slices for the cerebellum ($p < .001$ uncorrected, $k = 10$ voxels). CTRL, control condition; FEAT, feature condition; GEO, geometry condition; L, left hemisphere; OBJ, object condition; R, right hemisphere.
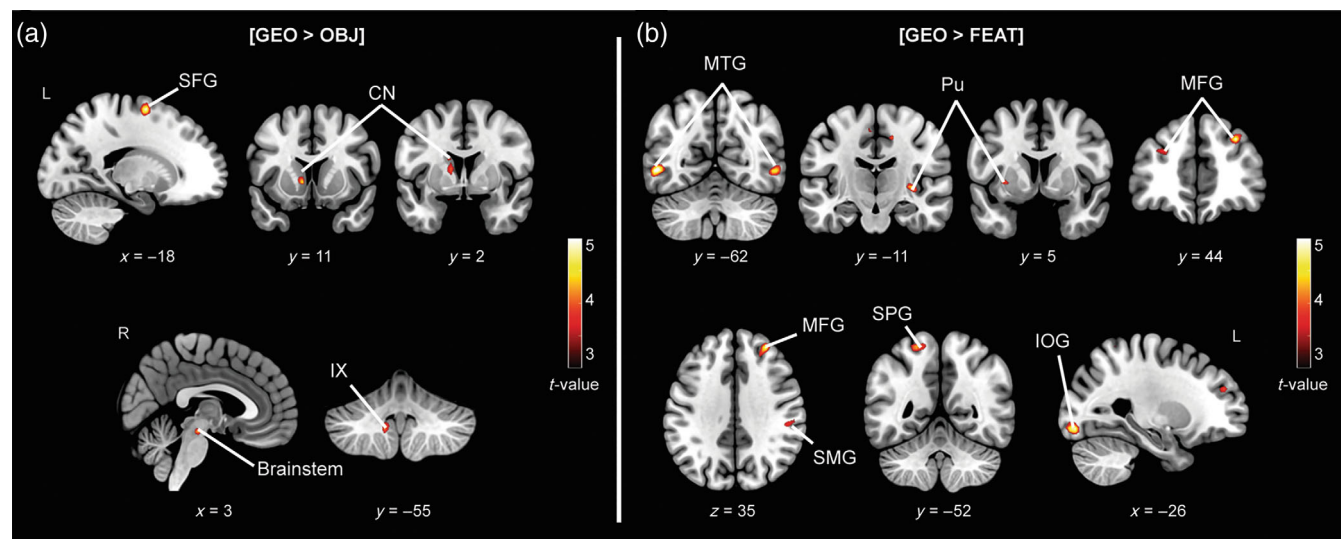


**FIGURE 4** Cerebral regions whose activity was elicited by the fMRI contrasts (a) [GEO > OBJ] and (b) [GEO > FEAT]. The neural activity is projected onto 2D slices ($p < .001$ uncorrected, $k = 10$ voxels). CN, caudate nucleus; FEAT, feature; GEO, geometry; IOG, inferior occipital gyrus; IX, lobule IX cerebellum; L, left hemisphere; MFG, middle frontal gyrus; MTG, middle temporal gyrus; OBJ, object; Pu, putamen; R, right hemisphere; SFG, superior frontal gyrus; SMG, supramarginal gyrus; SPG, superior parietal gyrus.
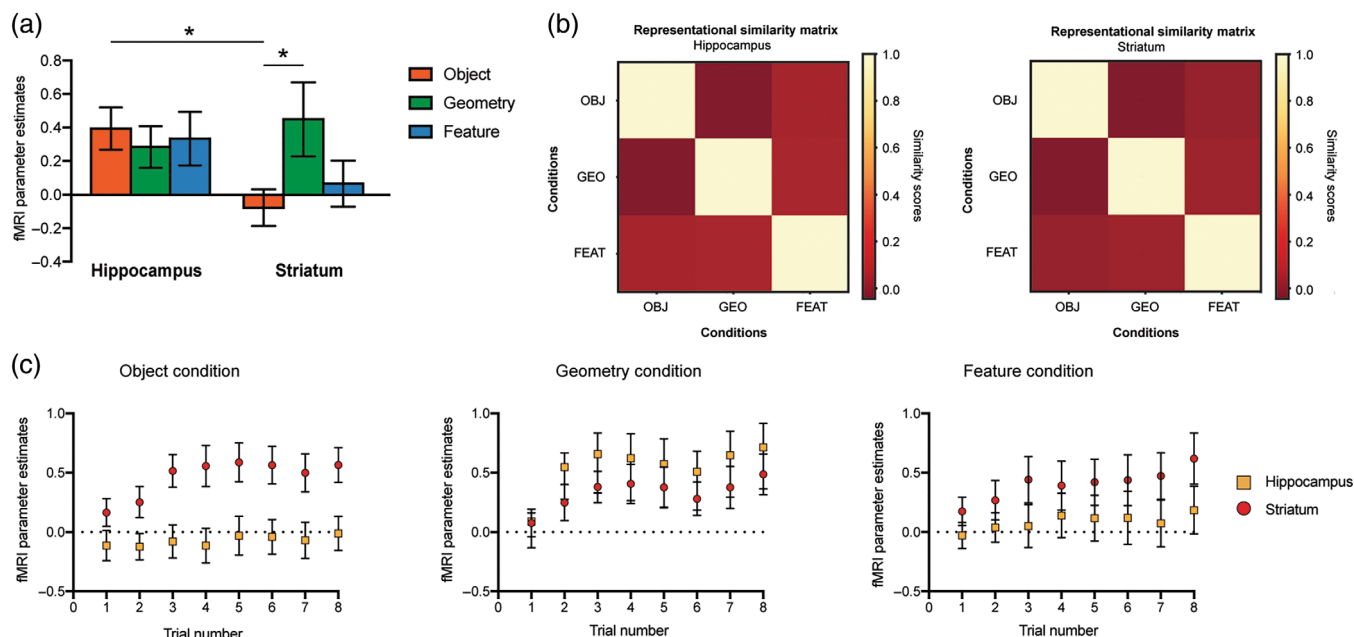
**FIGURE 5** Results of the ROI analyses. (a) FMRI parameter estimates in the bilateral hippocampus and striatum for the fMRI contrasts [OBJ > CTRL], [GEO > CTRL], and [FEAT > CTRL]. (b) Representational similarity matrices for the hippocampus (left) and striatum (right) averaged across subjects. Similarity scores are Fisher *z*-transformed Pearson correlation coefficients, and they represent the overlap in terms of neural patterns between the object, geometry, and feature conditions. (c) FMRI parameter estimates in the hippocampus and striatum for fMRI contrasts comparing neural activity in each trial of the object condition to that in one trial of the control condition (e.g., [OBJ t1 > CTRL t1]), neural activity in each trial of the geometry condition to that in one trial of the control condition (e.g., [GEO t1 > CTRL t1]) and neural activity in each trial of the feature condition to that in one trial of the control condition (e.g., [FEAT t1 > CTRL t1]). All error bars reflect standard errors of the mean.

rank correlations between hippocampal and striatal activity and navigation time in each condition. Finally, we examined anterior and posterior hippocampal activity. These complementary analyses revealed that there were no significant differences in fMRI parameter activity across conditions between the anterior and posterior hippocampi (Figure S3).

To complement the above univariate findings, we conducted representational similarity analyses aimed at investigating the similarity of multivoxel activations in the hippocampus and striatum between the object, geometry, and feature conditions. We found that the pairwise similarities between conditions were not significantly different from zero in the hippocampus and striatum (Figure 5b). We then performed a linear mixed-effects model to test the influence of ROI, condition pair and their interaction (ROI × condition pair) on neural similarities. No significant effects were found. Separate linear mixed-effects model analyses for the hippocampus and striatum further revealed that neural similarity patterns were not significantly explained by neither the object (hippocampus: $t = -1.49$, $p = .14$; striatum: $t = -0.84$, $p = .21$) nor the geometry theoretical models (hippocampus: $t = -1.44$, $p = .26$; striatum: $t = -0.31$, $p = .41$).

# 4 | DISCUSSION

Despite extensive knowledge surrounding the importance of visual information for spatial navigation, few studies have sought to elucidate how distinct types of visual spatial cues modulate behavior and

brain activity. In this study, we examined the neural activity associated with object-, geometry-, and feature-based spatial navigation in an unbiased, two-choice behavioral paradigm using univariate and multivariate fMRI analyses. Success rate was equivalent across the three conditions. However, we found that participants took longer to reach the goal in the geometry condition than in the object condition.

## 4.1 | A shared cerebral network for visual spatial cue processing

The whole-brain analyses revealed extended neural activations that were common to all conditions and that have been repeatedly implicated in spatial orientation paradigms (Chrastil, 2013; Cona & Scarpazza, 2019; Epstein et al., 2017; Qiu et al., 2019; Spiers & Barry, 2015). Unsurprisingly, multiple areas associated with visuospatial processing in the temporal and occipital lobes were activated. For example, the three conditions yielded activity in the fusiform gyrus, which may be reflecting the accurate recognition of novel information (Ewbank et al., 2005) and exemplifies the overarching importance of visual processing during fMRI virtual navigation tasks (Taube et al., 2013). We also noticed that the cerebellum was consistently activated, offering additional insight into its relevance for navigation (Iglói et al., 2015; Rochefort et al., 2013; Rondi-Reig et al., 2014).

While the above whole-brain results give us an idea of broad network similarities, the conjunction analysis revealed a more specific

overlap of the right anterior cingulate cortex (ACC) and the right inferior temporal cortex across conditions. The common engagement of the ACC can be interpreted in light of its function as an internal monitor (Carter et al., 1998; Walton et al., 2003; Wang et al., 2005). Indeed, the primate ACC is positioned at the crossroads between medial temporal structures and premotor regions allowing for the integration of affective and contextual memory information with goal-directed action (Botvinick et al., 2004; Hayden & Platt, 2010; Ito et al., 2003). In our experiment, reorientation required participants to notice their change of position within the maze and re-evaluate their trajectory accordingly. Lending credence to our result, Javadi et al. (2019) similarly found peak ACC activation when subjects understood that they had deviated from the optimal path and that they needed to backtrack (Javadi et al., 2019). The inferior temporal cortex is a central part of the ventral visual stream and it is critical for high-level visual processing such as perceptual detection and identification of faces, objects and scenes (Aguirre et al., 1998; Epstein et al., 1999; Grill-Spector & Weiner, 2014; Kanwisher, 2010; Kravitz et al., 2013; Landis et al., 1986; Litman et al., 2009). Together, these findings strengthen the argument for similarities between distinct forms of visual spatial cue processing for navigation.

## 4.2 | The specificity of processing geometric spatial cues

Although participants displayed optimal performance in all three conditions in terms of success rate (Figure 2a), our results emphasize a behavioral specificity for the processing of geometric cues compared with object and featural cues. Indeed, participants took longer to reach the goal in the geometry condition compared with the object condition and appeared to need more trials to reach optimal performance (Figure 2b,c). Several important points can be made. First, one can appreciate that the concept of geometry is less accessible in declarative memory than the concept of landmarks. In other words, it may have been easier for participants to be consciously aware of which visual spatial cues they were relying on in the object and feature conditions than in the geometry condition. Second, geometric information including angles between arms, lengths of corridors, and overall shape of the central area was available in the maze for participants to exploit. We speculate that this information was less noticeable and salient than both objects and features. The increased perceived difficulty of the geometry condition may provide an explanation for the differences in navigation time and learning curves.

The above behavioral results hint at the differential processing of geometric cues specifically and are corroborated by our fMRI whole-brain analyses. Indeed, our results highlight regional specificities for landmark- and geometry-based navigation. First, the whole-brain analyses revealed left hippocampal activity in the object and feature conditions only. It is important to emphasize that these results do not indicate an absence of hippocampal activity from the geometry condition, but rather that it is not significant compared with that in the other two conditions (see Section 3.3). Sutton et al. (2010) similarly reported increased hippocampal engagement in the presence of a distinctive featural cue embedded within environmental boundaries. We hypothesize that the saliency of object and featural cues enabled participants to better integrate local visual information with the broader spatial context into a unified hippocampal-dependent representation. In addition, the left lateralized activity reported is consistent with a previous study showing a specific role for the left hippocampus in spatial memory for object location (Miller et al., 2018). Second, directly contrasting the geometry condition with the object and feature conditions revealed striking disparities. In accordance with previous studies, geometry-based navigation yielded greater activity in a vast neural network comprising the frontal cortex, parietal cortex, and striatum (Forloines et al., 2019; Sutton et al., 2010, 2012). Both frontal and striatal regions are involved in the evaluation and selection of adequate behavior, and prefrontal inputs to the striatum could facilitate context-dependent and flexible navigational responses (Brown et al., 2012; Goodroe et al., 2018; Haber et al., 2006). The specific demand on frontal and striatal function for geometry processing may thus indicate more intricate decision-making processes attributable to the reduced saliency of geometric cues. Taken together, the above findings converge toward the idea that geometric cues in our paradigm are processed in a different manner to object and featural cues.

## 4.3 | Rethinking the concept of landmark in human spatial navigation

In fMRI studies, landmarks have been conceptualized as discrete objects (Doeller et al., 2008; Iaria et al., 2003; Janzen et al., 2008; Janzen & Van Turennout, 2004), abstract shapes (Baumann et al., 2010; Wegman et al., 2014), buildings (Wolbers & Büchel, 2005), and embedded visual information (Sutton et al., 2010). As previously emphasized by Mitchell et al. (2018), a pressing question remains as to how objects and features are considered by the brain and whether the field is correct in assuming their indistinguishability (Mitchell et al., 2018). Even though directly comparing the two conditions did not yield any significant activations, intriguing differences were noted when contrasting the two cue-based conditions individually to the control condition. First, object-based and feature-based navigation recruited distinct areas of the prefrontal cortex: the orbitofrontal gyrus and the superior frontal gyrus, respectively. While the orbitofrontal cortex is implicated in short-term memory for objects and is thought to mediate top-down visual recognition in association with temporal visual areas (Bar et al., 2006; Rolls, 2004), the superior frontal gyrus is more concerned with spatial working memory processing (Du Boisgueheneuc et al., 2006). The continuity of salient visual information with the environmental layout may thus activate regions oriented toward spatial processing rather than object processing. Second, we reported a more widespread pattern of activity comprising temporal and occipital regions during object-based navigation than during feature-based navigation. One can speculate that the integration of objects for spatial navigation requires fine-grained visual processing that is unnecessary to the use of salient colored walls

(i.e., features). Along those same lines, we showed activation of the anterior temporal pole when contrasting the object condition with the control condition. This result fits with the gradient nature of the medial temporal cortex with the most anterior part being concerned with the processing of objects and the most posterior part with that of scenes (Kravitz et al., 2013). It is worth noting that activation of the postcentral gyrus was observed during the feature condition and not the object condition. Rarely reported in spatial navigation studies, this structure has once been proposed to play a specific role in the processing of spatial layout and local environment cues from a self-centered perspective (Shelton & Gabrieli, 2002). Further accentuating the dichotomy between objects and features, representational similarity analyses revealed no significant correlations between the neural patterns subtending the two conditions in the hippocampus and striatum. Thus, despite objects and features bearing equivalent permanence and spatial utility, higher cognitive structures of the brain appear to treat them differently. What is typically considered to be a landmark may influence the underlying patterns of neural activity. Indeed, one could argue that objects and colored walls convey very different types of information in the real-world with the former being less stable and more frequently interacted with than the latter. Finally, the distinct occipital activations also underline the possibility that visual properties such as angular size or color contributed to the observed neural differences between objects and features. These results have important implications. We revealed that while objects and features can be used equally well to orient in space, object-based navigation is subtended by a more widespread pattern of temporal and occipital activations. One could thus speculate that featural information demands fewer cognitive resources for efficient spatial navigation. Future research should test whether favoring featural instead of object cues in architectural designs could facilitate spatial orientation in complex indoor spaces.

## 4.4 | Synergistic coactivation in the hippocampus and striatum

In light of the classic theory stating the existence of a hippocampal-dependent system for the representation of geometry and a striatal-dependent system for the representation of landmarks (Doeller et al., 2008; Doeller & Burgess, 2008), we conducted univariate and multivariate ROI analyses in the hippocampus and striatum. Interesting patterns emerged that we cautiously discuss below with a view to encourage further research. We observed equivalent ROI hippocampal activity in all three cue-based conditions and more striatal activity in the geometry condition. Moreover, representational similarity analyses revealed that the patterns of activity in the hippocampus and striatum were not specifically associated with the processing of either objects or geometry. We emphasize that this finding should be interpreted with caution as the absence of effect could be linked in part to methodological characteristics including voxel size and large ROIs. Notwithstanding, our results thus fail to support Doeller and colleagues' conclusions that two causally dissociable systems

(hippocampus-based and striatum-based) are associated with geometric and landmark cue processing, respectively. Multiple factors could account for such discrepant findings. First, in the virtual environment designed by Doeller et al. both proximal and distal landmarks were available whereas our environment only contained proximal landmarks. Several reports have highlighted the behavioral and neural differences linked to processing proximal or distal visual information when navigating (Hébert et al., 2017; Knierim & Hamilton, 2011). Second, we used highly divergent definitions of *geometric information*. In their experiment geometry was a circular boundary that could not be used in itself to orient while geometry in our experiment consisted of angles and wall lengths and could be used to orient. The openness of the environmental space also constitutes a plausible candidate to explain our results. Multiple studies have shown that barriers modify spatial navigation performance and fragment the representation of space (Han & Becker, 2014; He et al., 2019; Li & Klippel, 2016; Meilinger et al., 2016; Wang & Brockmole, 2003). Doeller et al.s' environment consisted of a large open field whereas our virtual maze was a closed space delimited by corridors. Finally, we advocate that these contradictory findings can be best understood by discarding the view that the human hippocampus and striatum are largely juxtaposed systems during spatial cue encoding for spatial navigation. There is long-standing knowledge from rodent studies that the hippocampus mediates the formation of cognitive map-like representations while the striatum is specifically involved with stimulus-outcome associations (Squire, 2004; White & McDonald, 2002). Yet, converging evidence from the animal and human literature supports intricate cooperation and competition between these two memory systems (Gahnstrom & Spiers, 2020; Packard & Goodman, 2013; Rinaldi et al., 2020; van de Ven et al., 2020). Critically, Packard and Goodman (2013) posited that the heterogeneity of the visual environment, defined by the presence of multiple visual cues, could modulate this competition by favoring one type of strategy over another, ultimately diminishing competitive interference. In our experiment, the homogeneity of the geometry condition may have enhanced stimulus-outcome learning by preventing some competition from the hippocampus, which could account for the presence of striatal activity. The latter may also provide an explanation for the longer navigation time observed during geometry-based navigation. On the other hand, the heterogeneity of the environments in the object and feature conditions may have ceased most competitive interference from the striatum.

## 5 | CONCLUSION AND PERSPECTIVES

Taken together, our results suggest that despite some shared activations in the inferior temporal and anterior cingulate gyri, each instance of cue-based navigation displays its specific neural signature and is subtended by complex hippocampo-striatal coactivations. Gaining a deeper understanding of the relationship between the hippocampus and the striatum during spatial navigation could provide a more definitive answer regarding their involvement in landmark versus geometry processing (Doeller et al., 2008; Doeller & Burgess, 2008; Schuck et al., 2015). Moreover, the divergence between object and feature

spatial coding stresses the importance of considering vision and spatial navigation as tightly interwoven systems and the need to reevaluate the concept of landmark in the field of human spatial navigation (Meister & Buffalo, 2016, 2018; Nau et al., 2018).

Multiple questions still remain regarding the complex interaction between the visual environment and the neural processing of visual spatial cues. Cognitive properties such as permanence and spatial utility were equivalent across conditions hinting at the possible contribution of lower-level processes (Mitchell et al., 2018). While the influence of visual properties on brain activity in sensory and navigationally-relevant regions such as the hippocampus is being thoroughly investigated in the context of natural scene perception (Aly et al., 2013; Dima et al., 2018; Ghodrati et al., 2016; Groen et al., 2013, 2017; Kaiser et al., 2019; Kauffmann et al., 2015; Seijdel et al., 2020), it has seldom been explored during active spatial navigation. Spatial frequency content, contrast amplitude, angular size, and position in the visual field may constitute interesting research avenues. Recent studies have revealed that age-related impairments in navigational abilities could be partially explained by the decline of information processing in early visual regions (Koch et al., 2020; Ramanoël et al., 2020). Therefore, specific modulations of these basic visual properties could stabilize or even improve navigation performance. To test such hypotheses, eye-tracking methods coupled to neuroimaging constitute promising tools to test whether oculomotor behavior changes as a function of visual spatial cue quality and type and can predict navigational behavior (Nau et al., 2018, 2020).

## AUTHOR CONTRIBUTIONS

Study design: Stephen Ramanoël, Alice Bizeul, Anthony Ozier-Lafontaine, Marcia Bécu, José-Alain Sahel, Christophe Habas, Angelo Arleo; Data acquisition: Stephen Ramanoël, Alice Bizeul; Data processing: Stephen Ramanoël, Marion Durteste, Alice Bizeul; Manuscript writing: Stephen Ramanoël, Marion Durteste, Marcia Bécu, Angelo Arleo.

## ACKNOWLEDGMENTS

## CONFLICT OF INTEREST

The authors declare that the research was conducted in the absence of any commercial or financial relationships that could be construed as a potential conflict of interest.

## DATA AVAILABILITY STATEMENT

The data that support the findings of this study are available on request from the corresponding author. The fMRI data are not publicly available due to privacy or ethical restrictions.

## ORCID

*Stephen Ramanoël* https://orcid.org/0000-0003-4735-1097

## REFERENCES

Aguirre, G. K., Zarahn, E., & D'Esposito, M. (1998). An area within human ventral cortex sensitive to "building" stimuli: Evidence and implications. *Neuron*, 21, 373–383. https://doi.org/10.1016/S0896-6273(00)80546-2

Aly, M., Ranganath, C., & Yonelinas, A. P. (2013). Detecting changes in scenes: The hippocampus is critical for strength-based perception. *Neuron*, 78, 1127–1137. https://doi.org/10.1016/j.neuron.2013.04.018

Auger, S. D., & Maguire, E. A. (2018). Dissociating landmark stability from orienting value using functional magnetic resonance imaging. *Journal of Cognitive Neuroscience*, 30, 698–713. https://doi.org/10.1162/jocn_a_01231

Auger, S. D., Zeidman, P., & Maguire, E. A. (2015). A central role for the retrosplenial cortex in de novo environmental learning. *eLife*, 4. https://doi.org/10.7554/eLife.09031

Bar, M., Kassam, K. S., Ghuman, A. S., Boshyan, J., Schmidt, A. M., Dale, A. M., Hämäläinen, M. S., Marinkovic, K., Schacter, D. L., Rosen, B. R., & Halgren, E. (2006). Top-down facilitation of visual recognition. *Proceedings of the National Academy of Sciences of the United States of America*, 103, 449–454. https://doi.org/10.1073/pnas.0507062103

Baumann, O., Chan, E., & Mattingley, J. B. (2010). Dissociable neural circuits for encoding and retrieval of object locations during active navigation in humans. *NeuroImage*, 49, 2816–2825. https://doi.org/10.1016/j.neuroimage.2009.10.021

Bécu, M., Sheynikhovich, D., Tatur, G., Agathos, C. P., Bologna, L. L., Sahel, J. A., & Arleo, A. (2020). Age-related preference for geometric spatial cues during real-world navigation. *Nature Human Behaviour*, 4, 88–99. https://doi.org/10.1038/s41562-019-0718-z

Botvinick, M. M., Cohen, J. D., & Carter, C. S. (2004). Conflict monitoring and anterior cingulate cortex: An update. *Trends in Cognitive Sciences*, 8, 539–546. https://doi.org/10.1016/j.tics.2004.10.003

Brown, T. I., Ross, R. S., Tobyne, S. M., & Stern, C. E. (2012). Cooperative interactions between hippocampal and striatal systems support flexible navigation. *NeuroImage*, 60(2), 1316–1330. https://doi.org/10.1016/j.neuroimage.2012.01.046

Bullens, J., Nardini, M., Doeller, C. F., Braddick, O., Postma, A., & Burgess, N. (2010). The role of landmarks and boundaries in the development of spatial memory. *Developmental Science*, 13, 170–180. https://doi.org/10.1111/j.1467-7687.2009.00870.x

Carter, C. S., Braver, T. S., Barch, D. M., Botvinick, M. M., Noll, D., & Cohen, J. D. (1998). Anterior cingulate cortex, error detection, and the online monitoring of performance. *Science*, 280, 747–749. https://doi.org/10.1126/science.280.5364.747

Cheng, K. (1986). A purely geometric module in the rat's spatial representation. *Cognition*, 23, 149–178. https://doi.org/10.1016/0010-0277(86)90041-7

Chrastil, E. R. (2013). Neural evidence supports a novel framework for spatial navigation. *Psychonomic Bulletin and Review*, 20, 208–227. https://doi.org/10.3758/s13423-012-0351-6

Cona, G., & Scarpazza, C. (2019). Where is the "where" in the brain? A meta-analysis of neuroimaging studies on spatial cognition. *Human Brain Mapping*, 40(6), 1867–1886. https://doi.org/10.1002/hbm.24496

Corsi, P. M. (1973). Human memory and the medial temporal region of the brain. *Dissertation Abstracts International*, 34, 891.

Dalton, M. A., McCormick, C., & Maguire, E. A. (2019). Differences in functional connectivity along the anterior-posterior axis of human hippocampal subfields. *NeuroImage*, 192, 38–51. https://doi.org/10.1016/j.neuroimage.2019.02.066

Dima, D. C., Perry, G., & Singh, K. D. (2018). Spatial frequency supports the emergence of categorical representations in visual cortex during natural scene perception. *NeuroImage*, 179, 102–116. https://doi.org/10.1016/j.neuroimage.2018.06.033

Doeller, C. F., & Burgess, N. (2008). Distinct error-correcting and incidental learning of location relative to landmarks and boundaries. *Proceedings of the National Academy of Sciences*, 105(15), 5909–5914. https://doi.org/10.1073/pnas.0711433105

Doeller, C. F., King, J. A., & Burgess, N. (2008). Parallel striatal and hippocampal systems for landmarks and boundaries in spatial memory. *Proceedings of the National Academy of Sciences*, 105(15), 5915–5920. https://doi.org/10.1073/pnas.0801489105

Du Boisgueheneuc, F., Levy, R., Volle, E., Seassau, M., Duffau, H., Kinkingnehun, S., Samson, Y., Zhang, S., & Dubois, B. (2006). Functions of the left superior frontal gyrus in humans: A lesion study. *Brain*, 129, 3315–3328. https://doi.org/10.1093/brain/awl244

Ekstrom, A. D. (2015). Why vision is important to how we navigate. *Hippocampus*, 25(6), 731–735. https://doi.org/10.1002/HIPO.22449

Epstein, R., Harris, A., Stanley, D., & Kanwisher, N. (1999). The parahippocampal place area: Recognition, navigation, or encoding? *Neuron*, 23, 115–125. https://doi.org/10.1016/S0896-6273(00)80758-8

Epstein, R. A., Patai, E. Z., Julian, J. B., & Spiers, H. J. (2017). The cognitive map in humans: Spatial navigation and beyond. *Nature Neuroscience*, 20(11), 1504–1513. https://doi.org/10.1038/nn.4656

Epstein, R. A., & Vass, L. K. (2014). Neural systems for landmark-based wayfinding in humans. *Philosophical Transactions of the Royal Society B: Biological Sciences*, 369(1635), 20120533. https://doi.org/10.1098/rstb.2012.0533

Ewbank, M. P., Schluppeck, D., & Andrews, T. J. (2005). fMR-adaptation reveals a distributed representation of inanimate objects and places in human visual cortex. *NeuroImage*, 28, 268–279. https://doi.org/10.1016/j.neuroimage.2005.06.036

Fan, L., Li, H., Zhuo, J., Zhang, Y., Wang, J., Chen, L., Yang, Z., Chu, C., Xie, S., Laird, A. R., Fox, P. T., Eickhoff, S. B., Yu, C., & Jiang, T. (2016). The Human Brainnetome Atlas: A new brain atlas based on connectional architecture. *Cerebral Cortex*, 26, 3508–3526. https://doi.org/10.1093/cercor/bhw157

Folstein, M. R., Folstein, S. E., & McHugh, P. R. (1975). "Mini-mental state". A practical method for grading the cognitive state of patients for the clinician. *Journal of Psychiatric Research*, 12(3), 189–198. https://doi.org/10.1016/0022-3956(75)90026-6

Forloines, M. R., Reid, M. A., Thompkins, A. M., Robinson, J. L., & Katz, J. S. (2019). Neurofunctional correlates of geometry and feature use in a virtual environment. *Journal of Experimental Psychology: Learning Memory and Cognition*, 45, 1347–1363. https://doi.org/10.1037/xlm0000656

Friston, K. J., Holmes, A. P., Poline, J. B., Grasby, P. J., Williams, S. C. R., Frackowiak, R. S. J., & Turner, R. (1995). Analysis of fMRI time-series revisited. *NeuroImage*, 2, 45–53. https://doi.org/10.1006/nimg.1995.1007

Gahnstrom, C. J., & Spiers, H. J. (2020). Striatal and hippocampal contributions to flexible navigation in rats and humans. *Brain and Neuroscience Advances*, 4. https://doi.org/10.1177/2398212820979772

Gallistel, C. R. (1990). *The organization of learning*. Bradford Books/MIT Press.

Ghodrati, M., Ghodousi, M., & Yoonessi, A. (2016). Low-level contrast statistics of natural images can modulate the frequency of event-related potentials (ERP) in humans. *Frontiers in Human Neuroscience*, 10, 630. https://doi.org/10.3389/fnhum.2016.00630

Goodroe, S. C., Starnes, J., & Brown, T. I. (2018). The complex nature of hippocampal-striatal interactions in spatial navigation. *Frontiers in Human Neuroscience*, 12, 250. https://doi.org/10.3389/fnhum.2018.00250

Gouteux, S., Thinus-Blanc, C., & Vauclair, J. (2001). Rhesus monkeys use geometric and nongeometric information during a reorientation task. *Journal of Experimental Psychology: General*, 130(3), 505–519. https://doi.org/10.1037/0096-3445.130.3.505

Gouteux, S., & Spelke, E. S. (2001). Children's use of geometry and landmarks to reorient in an open space. *Cognition*, 81, 119–148. https://doi.org/10.1016/S0010-0277(01)00128-7

Grill-Spector, K., & Weiner, K. S. (2014). The functional architecture of the ventral temporal cortex and its role in categorization. *Nature Reviews Neuroscience*, 15, 536–548. https://doi.org/10.1038/nrn3747

Groen, I. I. A., Ghebreab, S., Prins, H., Lamme, V. A. F., & Steven Scholte, H. (2013). From image statistics to scene gist: Evoked neural activity reveals transition from low-level natural image structure to scene category. *Journal of Neuroscience*, 33, 18814–18824. https://doi.org/10.1523/JNEUROSCI.3128-13.2013

Groen, I. I. A., Silson, E. H., & Baker, C. I. (2017). Contributions of low- and high-level properties to neural processing of visual scenes in the human brain. *Philosophical Transactions of the Royal Society B: Biological Sciences*, 33(48), 18814–18824. https://doi.org/10.1098/rstb.2016.0102

Haber, S. N., Kim, K. S., Mailly, P., & Calzavara, R. (2006). Reward-related cortical inputs define a large striatal region in primates that interface with associative cortical connections, providing a substrate for incentive-based learning. *Journal of Neuroscience*, 26, 8368–8376. https://doi.org/10.1523/JNEUROSCI.0271-06.2006

Han, X., & Becker, S. (2014). One spatial map or many? Spatial coding of connected environments. *Journal of Experimental Psychology: Learning Memory and Cognition*, 40(2), 511–531. https://doi.org/10.1037/a0035259

Hayden, B. Y., & Platt, M. L. (2010). Neurons in anterior cingulate cortex multiplex information about reward and action. *Journal of Neuroscience*, 30, 3339–3346. https://doi.org/10.1523/JNEUROSCI.4874-09.2010

He, Q., McNamara, T. P., & Brown, T. I. (2019). Manipulating the visibility of barriers to improve spatial navigation efficiency and cognitive mapping. *Scientific Reports*, 9, 11567. https://doi.org/10.1038/s41598-019-48098-0

Hébert, M., Bulla, J., Vivien, D., & Agin, V. (2017). Are distal and proximal visual cues equally important during spatial learning in mice? A pilot study of overshadowing in the spatial domain. *Frontiers in Behavioral Neuroscience*, 11, 109. https://doi.org/10.3389/fnbeh.2017.00109

Hermer, L., & Spelke, E. (1996). Modularity and development: The case of spatial reorientation. *Cognition*, 61, 195–232. https://doi.org/10.1016/S0010-0277(96)00714-7

Hupbach, A., & Nadel, L. (2005). Reorientation in a rhombic environment: No evidence for an encapsulated geometric module. *Cognitive Development*, 20, 279–302. https://doi.org/10.1016/j.cogdev.2005.04.003

Iaria, G., Petrides, M., Dagher, A., Pike, B., & Bohbot, V. D. (2003). Cognitive strategies dependent on the hippocampus and caudate nucleus in human navigation: Variability and change with practice. *The Journal of Neuroscience*, 23, 5945–5952.

Iglói, K., Doeller, C. F., Paradis, A. L., Benchenane, K., Berthoz, A., Burgess, N., & Rondi-Reig, L. (2015). Interaction between hippocampus and cerebellum crusi in sequence-based but not place-based navigation. *Cerebral Cortex*, 25, 4146–4154. https://doi.org/10.1093/cercor/bhu132

Ito, S., Stuphorn, V., Brown, J. W., & Schall, J. D. (2003). Performance monitoring by the anterior cingulate cortex during saccade countermanding. *Science*, 302, 120–122. https://doi.org/10.1126/science.1087847

Janzen, G., Jansen, C., & Van Turennout, M. (2008). Memory consolidation of landmarks in good navigators. *Hippocampus*, 18, 40–47. https://doi.org/10.1002/hipo.20364

Janzen, G., & Van Turennout, M. (2004). Selective neural representation of objects rellevant for navigation. *Nature Neuroscience*, 7, 673–677. https://doi.org/10.1038/nn1257

Javadi, A.-H., Patai, E. Z., Marin-Garcia, E., Margois, A., Tan, H.-R. M., Kumaran, D., Nardini, M., Penny, W., Duzel, E., Dayan, P., & Spiers, H. J. (2019). Backtracking during navigation is correlated with enhanced anterior cingulate activity and suppression of alpha oscillations and the "default-mode" network. *Proceedings of the Royal Society B: Biological Sciences*, 286, 20191016. https://doi.org/10.1098/rspb.2019.1016

Julian, J. B., Keinath, A. T., Marchette, S. A., & Epstein, R. A. (2018). The neurocognitive basis of spatial reorientation. *Current Biology*, *28*, R1059–R1073. https://doi.org/10.1016/j.cub.2018.04.057

Kaiser, D., Quek, G. L., Cichy, R. M., & Peelen, M. V. (2019). Object vision in a structured world. *Trends in Cognitive Sciences*, *23*, 672–685. https://doi.org/10.1016/j.tics.2019.04.013

Kanwisher, N. (2010). Functional specificity in the human brain: A window into the functional architecture of the mind. *Proceedings of the National Academy of Sciences of the United States of America*, *107*, 11163–11170. https://doi.org/10.1073/pnas.1005062107

Kauffmann, L., Ramanoël, S., Guyader, N., Chauvin, A., & Peyrin, C. (2015). Spatial frequency processing in scene-selective cortical regions. *NeuroImage*, *112*, 86–95. https://doi.org/10.1016/j.neuroimage.2015.02.058

Keinath, A. T., Julian, J. B., Epstein, R. A., & Muzzio, I. A. (2017). Environmental Geometry Aligns the Hippocampal Map during Spatial Reorientation. *Current biology : CB*, *27*(3), 309–317. https://doi.org/10.1016/j.cub.2016.11.046

Knierim, J. J., & Hamilton, D. A. (2011). Framing spatial cognition: Neural representations of proximal and distal frames of reference and their roles in navigation. *Physiological Reviews*, *91*, 1245–1279. https://doi.org/10.1152/physrev.00021.2010

Koch, C., Li, S. C., Polk, T. A., & Schuck, N. W. (2020). Effects of aging on encoding of walking direction in the human brain. *Neuropsychologia*, *141*, 107379. https://doi.org/10.1016/j.neuropsychologia.2020.107379

Kozhevnikov, M., & Hegarty, M. (2001). A dissociation between object manipulation spatial ability and spatial orientation ability. *Memory and Cognition*, *29*, 745–756. https://doi.org/10.3758/BF03200477

Kravitz, D. J., Saleem, K. S., Baker, C. I., Ungerleider, L. G., & Mishkin, M. (2013). The ventral visual pathway: An expanded neural framework for the processing of object quality. *Trends in Cognitive Sciences*, *17*, 26–49. https://doi.org/10.1016/j.tics.2012.10.011

Lagrené, K., Bécu, M., Seiple, W. H., Raphanel Bataille, M., Combariza, S., Paques, M., Aubois, A., Duclos, B., Eandi, C., Girmens, J.-F., Mohand-Said, S., & Arleo, A. (2019). Healthy and pathological visual aging in a French follow-up cohort study. *Investigative Ophthalmology & Visual Science*, *60*, 5915.

Landis, T., Cummings, J. L., Benson, D. F., & Palmer, E. P. (1986). Loss of topographic familiarity: An environmental agnosia. *Archives of Neurology*, *43*, 132. https://doi.org/10.1001/archneur.1986.00520020026011

Learmonth, A. E., Newcombe, N. S., Sheridan, N., & Jones, M. (2008). Why size counts: Children's spatial reorientation in large and small enclosures: Paper. *Developmental Science*, *11*, 414–426. https://doi.org/10.1111/j.1467-7687.2008.00686.x

Lee, S. A., & Spelke, E. S. (2010). Two systems of spatial representation underlying navigation. *Experimental Brain Research*, *210*(2), 179–188. https://doi.org/10.1007/s00221-010-2349-5

Lew, A. R. (2011). Looking beyond the boundaries: Time to put landmarks back on the cognitive map? *Psychological Bulletin*, *137*, 484–507. https://doi.org/10.1037/a0022315

Li, R., & Klippel, A. (2016). Wayfinding behaviors in complex buildings: The impact of environmental legibility and familiarity. *Environment and Behavior*, *48*(3), 482–510. https://doi.org/10.1177/0013916514550243

Litman, L., Awipi, T., & Davachi, L. (2009). Category-specificity in the human medial temporal lobe cortex. *Hippocampus*, *19*, 308–319. https://doi.org/10.1002/hipo.20515

Lourenco, S. F., Addy, D., & Huttenlocher, J. (2009). Location representation in enclosed spaces: What types of information afford young children an advantage? *Journal of Experimental Child Psychology*, *104*(3), 313–325. https://doi.org/10.1016/j.jecp.2009.05.007

Lowe, M. X., Rajsic, J., Gallivan, J. P., Ferber, S., & Cant, J. S. (2017). Neural representation of geometry and surface properties in object and scene perception. *NeuroImage*, *157*, 586–597. https://doi.org/10.1016/j.neuroimage.2017.06.043

Marchette, S. A., Vass, L. K., Ryan, J., & Epstein, R. A. (2015). Outside looking in: Landmark generalization in the human navigational system. *Journal of Neuroscience*, *35*, 14896–14908. https://doi.org/10.1523/JNEUROSCI.2270-15.2015

Meilinger, T., Strickrodt, M., & Bülthoff, H. H. (2016). Qualitative differences in memory for vista and environmental spaces are caused by opaque borders, not movement or successive presentation. *Cognition*, *155*, 77–95. https://doi.org/10.1016/j.cognition.2016.06.003

Meister, M. L. R., & Buffalo, E. A. (2016). Getting directions from the hippocampus: The neural connection between looking and memory. *Neurobiology of Learning and Memory*, *134*, 135–144. https://doi.org/10.1016/j.nlm.2015.12.004

Meister, M. L. R., & Buffalo, E. A. (2018). Neurons in primate entorhinal cortex represent gaze position in multiple spatial reference frames. *Journal of Neuroscience*, *38*, 2430–2441. https://doi.org/10.1523/JNEUROSCI.2432-17.2018

Miller, J., Watrous, A. J., Tsitsiklis, M., Lee, S. Ah., Sheth, S. A., Schevon, C. A., Smith, E. H., Sperling, M. R., Sharan, A., Asadi-Pooya, A. A., Worrell, G. A., Meisenhelter, S., Inman, C. S., Davis, K. A., Lega, B., Wanda, P. A., Das, Das, Stein, J. M., Gorniak, R., & Jacobs, J. (2018). Lateralized hippocampal oscillations underlie distinct aspects of human spatial memory and navigation. *Nature Communications 9*, 2423. https://doi.org/10.1038/s41467-018-04847-9

Mitchell, A. S., Czajkowski, R., Zhang, N., Jeffery, K., & Nelson, A. J. D. (2018). Retrosplenial cortex and its role in spatial cognition. *Brain and Neuroscience Advances*, *2*. https://doi.org/10.1177/2398212818757098

Nau, M., Navarro Schröder, T., Bellmund, J. L. S., & Doeller, C. F. (2018). Hexadirectional coding of visual space in human entorhinal cortex. *Nature Neuroscience*, *21*, 188–190. https://doi.org/10.1038/s41593-017-0050-8

Nau, M., Navarro Schröder, T., Frey, M., & Doeller, C. F. (2020). Behavior-dependent directional tuning in the human visual-navigation network. *Nature Communications*, *11*, 3247. https://doi.org/10.1038/s41467-020-17000-2

Packard, M. G., & Goodman, J. (2013). Factors that influence the relative use of multiple memory systems. *Hippocampus*, *23*, 1044–1052. https://doi.org/10.1002/hipo.22178

Qiu, Y., Wu, Y., Liu, R., Wang, J., Huang, H., & Huang, R. (2019). Representation of human spatial navigation responding to input spatial information and output navigational strategies: An ALE meta-analysis. *Neuroscience and Biobehavioral Reviews*, *103*, 60–72. https://doi.org/10.1016/j.neubiorev.2019.06.012

Ramanoël, S., Durteste, M., Bécu, M., Habas, C., & Arleo, A. (2020). Differential brain activity in regions linked to visuospatial processing during landmark-based navigation in young and healthy older adults. *Frontiers in Human Neuroscience*, *14*, 1–16. https://doi.org/10.3389/fnhum.2020.552111

Reichert, J. F., & Kelly, D. M. (2011). Use of local and global geometry from object arrays by adult humans. *Behavioural Processes*, *86*(2), 196–205. https://doi.org/10.1016/j.beproc.2010.11.008

Rinaldi, A., De Leonibus, E., Cifra, A., Torromino, G., Minicocci, E., De Sanctis, E., Lopez-Pedrajas, R. M., Oliverio, A., & Mele, A. (2020). Flexible use of allocentric and egocentric spatial memories activates differential neural networks in mice. *Scientific Reports*, *10*(1), 11338. https://doi.org/10.1038/s41598-020-068025-y

Rochefort, C., Lefort, J., & Rondi-Reig, L. (2013). The cerebellum: A new key structure in the navigation system. *Frontiers in Neural Circuits*, *7*, 35. https://doi.org/10.3389/fncir.2013.00035

Rolls, E. T. (2004). The functions of the orbitofrontal cortex. *Brain and Cognition*, *55*, 11–29. https://doi.org/10.1016/S0278-2626(03)00277-X

Rondi-Reig, L., Paradis, A. L., Lefort, J. M., Babayan, B. M., & Tobin, C. (2014). How the cerebellum may monitor sensory information for spatial representation. *Frontiers in Systems Neuroscience*, *8*, 205. https://doi.org/10.3389/fnsys.2014.00205

Schuck, N. W., Doeller, C. F., Polk, T. A., Lindenberger, U., & Li, S. C. (2015). Human aging alters the neural computation and representation

of space. *NeuroImage*, *117*, 141–150. https://doi.org/10.1016/j.neuroimage.2015.05.031

Seijdel, N., Jahfari, S., Groen, I. I. A., & Scholte, H. S. (2020). Low-level image statistics in natural scenes influence perceptual decision-making. *Scientific Reports*, *10*, 10573. https://doi.org/10.1038/s41598-020-67661-8

Shelton, A. L., & Gabrieli, J. D. E. (2002). Neural correlates of encoding space from route and survey perspectives. *Journal of Neuroscience*, *22*, 2711–2717. https://doi.org/10.1523/jneurosci.22-07-02711.2002

Sheynikhovich, D., Chavarriaga, R., Strösslin, T., Arleo, A., & Gerstner, W. (2009). Is there a geometric module for spatial orientation? Insights from a rodent navigation model. *Psychological Review*, *116*(3), 540–566. https://doi.org/10.1037/a0016170

Spiers, H. J., & Barry, C. (2015). Neural systems supporting navigation. *Current Opinion in Behavioral Sciences*, *1*, 47–55. https://doi.org/10.1016/j.cobeha.2014.08.005

Squire, L. R. (2004). Memory systems of the brain: A brief history and current perspective. *Neurobiology of Learning and Memory*, *82*, 171–177. https://doi.org/10.1016/j.nlm.2004.06.005

Stankiewicz, B. J., & Kalia, A. A. (2007). Acquisition of structural versus object landmark knowledge. *Journal of Experimental Psychology: Human Perception and Performance*, *33*, 378–390. https://doi.org/10.1037/0096-1523.33.2.378

Sutton, J. E., Joanisse, M. F., & Newcombe, N. S. (2010). Spinning in the scanner: Neural correlates of virtual reorientation. *Journal of Experimental Psychology: Learning Memory and Cognition*, *36*, 1097–1107. https://doi.org/10.1037/a0019938

Sutton, J. E., & Newcombe, N. S. (2014). The hippocampus is not a geometric module: Processing environment geometry during reorientation. *Frontiers in Human Neuroscience*, *8*(August), 1–6. https://doi.org/10.3389/fnhum.2014.00596

Sutton, J. E., Twyman, A. D., Joanisse, M. F., & Newcombe, N. S. (2012). Geometry three ways: An fMRI investigation of geometric information processing during reorientation. *Journal of Experimental Psychology: Learning Memory and Cognition*, *38*(6), 1530–1541. https://doi.org/10.1037/a0028456

Taube, J. S., Valerio, S., & Yoder, R. M. (2013). Is navigation in virtual reality with fMRI really navigation? *Journal of Cognitive Neuroscience*, *25*(7), 1008–1019. https://doi.org/10.1162/jocn_a_00386

Tzourio-Mazoyer, N., Landeau, B., Papathanassiou, D., Crivello, F., Etard, O., Delcroix, N., Mazoyer, B., & Joliot, M. (2002). Automated anatomical labeling of activations in SPM using a macroscopic anatomical parcellation of the MNI MRI single-subject brain. *NeuroImage*, *15*, 273–289. https://doi.org/10.1006/nimg.2001.0978

van de Ven, V., Lee, C., Lifanov, J., Kochs, S., Jansma, H., & De Weerd, P. (2020). Hippocampal-striatal functional connectivity supports processing of temporal expectations from associative memory. *Hippocampus*, *30*, 926–937. https://doi.org/10.1002/hipo.23205

Vandenberg, S. G., & Kuse, A. R. (1978). Mental rotations, a group test of three-dimensional spatial visualization. *Perceptual and Motor Skills*, *47*(2), 599–604. https://doi.org/10.2466/pms.1978.47.2.599

Walton, M. E., Bannerman, D. M., Alterescu, K., & Rushworth, M. F. S. (2003). Functional specialization within medial frontal cortex of the anterior cingulate for evaluating effort-related decisions. *Journal of Neuroscience*, *23*, 6475–6479. https://doi.org/10.1523/jneurosci.23-16-06475.2003

Wang, C., Ulbert, I., Schomer, D. L., Marinkovic, K., & Halgren, E. (2005). Responses of human anterior cingulate cortex microdomains to error detection, conflict monitoring, stimulus-response mapping, familiarity, and orienting. *Journal of Neuroscience*, *25*, 604–613. https://doi.org/10.1523/JNEUROSCI.4151-04.2005

Wang, R. F., & Brockmole, J. R. (2003). Human navigation in nested environments. *Journal of Experimental Psychology: Learning Memory and Cognition*, *29*(3), 398–404. https://doi.org/10.1037/0278-7393.29.3.398

Wegman, J., Tyborowska, A., & Janzen, G. (2014). Encoding and retrieval of landmark-related spatial cues during navigation: An fMRI study. *Hippocampus*, *24*, 853–868. https://doi.org/10.1002/hipo.22275

Weiskopf, N., Hutton, C., Josephs, O., & Deichmann, R. (2006). Optimal EPI parameters for reduction of susceptibility-induced BOLD sensitivity losses: A whole-brain analysis at 3 T and 1.5 T. *NeuroImage*, *33*(2), 493–504. https://doi.org/10.1016/j.neuroimage.2006.07.029

White, N. M., & McDonald, R. J. (2002). Multiple parallel memory systems in the brain of the rat. *Neurobiology of Learning and Memory*, *77*, 125–184. https://doi.org/10.1006/nlme.2001.4008

Wolbers, T., & Büchel, C. (2005). Dissociable retrosplenial and hippocampal contributions to successful formation of survey representations. *Journal of Neuroscience*, *25*, 3333–3340. https://doi.org/10.1523/JNEUROSCI.4705-04.2005

Wolbers, T., & Hegarty, M. (2010). What determines our navigational abilities? *Trends in Cognitive Sciences*, *14*(3), 138–146. https://doi.org/10.1016/J.TICS.2010.01.001

Zeidman, P., & Maguire, E. A. (2016). Anterior hippocampus: The anatomy of perception, imagination and episodic memory. *Nature Reviews. Neuroscience*, *17*(3), 173–182. https://doi.org/10.1038/NRN.2015.24

## SUPPORTING INFORMATION

Additional supporting information can be found online in the Supporting Information section at the end of this article.